Shear induced smectic-A–smectic-C transition in side-chain liquid-crystalline polymers

Laurence Noirez

Shear Induced Smectic-*A*–Smectic-*C* Transition in Side-Chain Liquid-Crystalline Polymers

Laurence Noirez
Laboratoire Léon Brillouin (CEA-CNRS), Ce-Saclay, 91191 Gif-sur-Yvette, France
(Received 5 August 1999)

We show that the smectic layer orientation in side-chain liquid-crystalline polymers depends on the molecular weight and the shear rate. Parallel orientation is obtained with the low molecular weight polymer and reveals a shear induced decrease of the smectic layer thickness. In contrast with usual liquid crystals, the shear torque acts at the mesogen scale through an efficient coupling between the polymer main chain and the mesogens resulting in a smectic-*A*–smectic-*C* transition.

PACS numbers: 61.30.–v, 47.50.+d, 64.70.Md

Changes at a mesoscopic scale are a characteristic response of both small molecule liquid crystals and liquid-crystalline polymers to shear flow. This feature is particularly true in the case of the smectic phase because of the strength of the liquid crystalline field. The viscous torque exercised by the smectic arrangement eliminates all possibility of flow aligning behavior, and the low energy solutions consist either of a distribution of the smectic layers in concentric cylinders as observed for both small molecules [1] and liquid-crystalline polymers [2] or a reorientation of the director usually towards the neutral axis, but sometimes also to the velocity gradient axis $\vec{\nabla} \cdot \vec{v}$ [3].

In the following, we will mainly focus on the latter situation where the smectic layers adopt the parallel orientation; i.e., the director is oriented parallel to the velocity gradient. In the case of side-chain liquid-crystalline polymers (SCLCPs) where the polymer main chains occupy preferentially the interfaces between the mesogenic layers, a parallel orientation has been found [3]. This shear induced orientation is associated with a uniaxial elongation of the main chains along the velocity direction $\vec{v}$. This main-chain elongation contrasts with the elongated tilted shape displayed by usual polymers [4] and results from the slip motion of the smectic planes [3]. This feature is not the only striking aspect of the SCLCPs rheology. Very accurate measurements on the smectic structure under flow reveal an unexpected shear induced decrease of the layer thickness. To our knowledge, such a phenomenon has never been observed. For low molecular weight thermotropic liquid crystals, a dilatation of the layers due to the development of shear induced instabilities is even expected.

The LC polymer chosen, PMA-OC_4H_9, corresponds to this chemical formula:

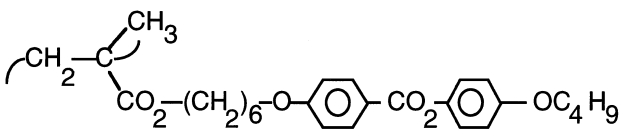

and displays the following phase succession: T_g-38 °C-S_{A1}-106 °C-*N*-113 °C-*I*.

The structure, the main chain, and the smectic order parameters are detailed in [5,6]. As stated above, the behavior under shear flow was already explored for the polymer of molecular weight 25 700 and polydispersity of 2.2 (determined by gel permeation chromatography-light scattering on line at the ICS Strasbourg), using neutron scattering techniques.

The sample was placed in a specific neutron setup which allows the observation of smectic layers lying in the $(\vec{v}, \vec{z})$ plane, thus in the parallel orientation. It consists of a thin hollow open aluminum ring above which a solid ring in contact with the polymer is rotating [3(b)]. Because of its high instrumental resolution and of the absence of inelastic contribution (measure of the elastic signal alone), the neutron spectrometer chosen to characterize the position, width, and intensity of the smectic reflection is a three-axis spectrometer. Since this spectrometer scans only the horizontal plane, the shear cell ring was placed vertically. So, the incident beam, crossing one ring side (coinciding with the center of the reciprocal space) scans the two axes contained in the horizontal plane which are the velocity-gradient $\vec{\nabla} \cdot \vec{v}$ axis and the neutral axis $\vec{z}$ (Fig. 1). The wavelength was 4.18 Å. Distances obtained with the 2D small-angle neutron scattering multidetector PAXY have also been added. In this case, the incident beam is along the neutral axis $\vec{z}$ and crosses the shear cell tilted at 2°–3° to the horizontal so that one side intercepts the beam; the 2D multidetector explores the plane containing the velocity and the velocity gradient $(\vec{v}, \vec{\nabla} \cdot \vec{v})$ [as already described elsewhere [3(b)]]. Finally, for the perpendicular orientation, only the 2D multidetector was employed to access as described in [3(a)] to the $(\vec{v}, \vec{z})$ plane. In this case the incident beam is along the velocity gradient $\vec{\nabla} \cdot \vec{v}$ axis. The scattering conditions were 4 Å wavelength and 1.5 m sample-multidetector distance. The experiment started by heating the sample to the isotropic phase to erase all previous orientations and ensure the homogeneity of the sample. The temperature was then decreased down to 5–10 °C below to the N-S_A transition to keep sufficient viscoelastic properties (at lower temperature, the solidlike properties dominate). A continuous steady-state shear was then applied by increasing slowly the shear rate from 0.1 to 50 s^{-1}.

In the absence of external constraint, the polymer shows a 001 smectic reflection characterized by an increase of the

 0031-9007/00/84(10)/2164(4)$15.00

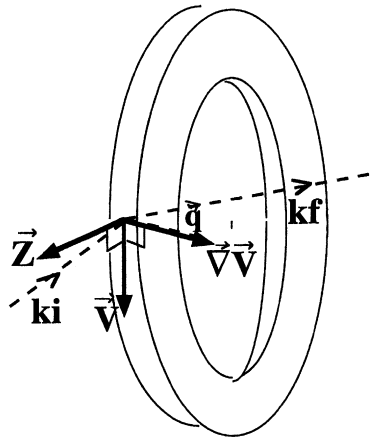

FIG. 1. Section of the shear cell ring (placed in a vertical position for the three-axis geometry) defining the three axes $(\vec{v}, \vec{\nabla} \cdot \vec{v}, \vec{z})$. The scattering vector is defined by $\vec{q} = \vec{k}_i - \vec{k}_f$, where $\vec{k}_i$ is the incident beam and $\vec{k}_f$ is the diffracted one.

intensity [5(a),6(a)] and of the layer thickness [Fig. 2(a)] as the temperature decreases. The layer thickness increases about 0.5% for a temperature decrease of 50°. This variation is usually explained by an increase of the mesogen length due, in particular, to a mobility loss and thus an ordering of the alkyl part of the mesogen. This layer thickness corresponds to the most extended side-chain configuration forming thus a monolayer S_{A1} phase; it is a "rigid" smectic *A* phase. Any interpretation owing to partially bilayer modulations or smectic-*C* tendency will be thus excluded.

Under shear flow, in the high temperature smectic phase ($T = 95\,^{\circ}\mathrm{C}$), the orientation is parallel and the intensity maximum of the 001 smectic reflection evolves as a function of the shear rate as described in Fig. 2(b). As already noticed [3(b)], a plateau is reached at low shear rates ($\dot{\gamma} \approx 1\ \mathrm{s}^{-1}$). It corresponds to the establishment of the macroscopic orientation which orients the director $\vec{n}$ parallel to the $\vec{\nabla} \cdot \vec{v}$ axis. A second regime develops above a critical shear rate ($\dot{\gamma}_c \approx 22\ \mathrm{s}^{-1}$ at 95 °C) which gives rise to an intensity close to the unoriented state (thus a destruction of the previous orientation). In contrast, no particular change can be observed in the shape of the peak on the plane $(\vec{v}, \vec{z})$; i.e., the mosaicity ω and the correlation length $\xi_{\parallel}$ along the director remain unchanged (Fig. 3) during the shear process. Concerning the variation of the layer distance d, which is a measure independent of ω and $\xi_{\parallel}$, a critical shear rate similar to the one observed for the intensity separates two regimes of layer thickness [Fig. 2(b)]. At low shear rates ($0 < \dot{\gamma} < 20\ \mathrm{s}^{-1}$), one observes a continuous decrease of the smectic layer distance followed by a second regime for which a substantial increase of the layer thickness occurs. It is clear that the second regime corresponds to a relaxation state. The expected value at rest at 95 °C is $d \approx 28.75 \pm 0.02$ Å. Compared to this value, Fig. 2(b) indicates that the thickness decrease is achieved as soon as the smallest shear rate; for $\dot{\gamma}_0 \approx 0.1\ \mathrm{s}^{-1}$, $d \approx 28.5$ Å which represents a variation of 0.9% of the total thickness. This small variation actually represents a huge constraint in bulky systems. By increasing the shear, the layer distance follows a power law decrease until it reaches its lowest value $d \approx 28.15$ Å for $\dot{\gamma}_0 \approx 18\text{–}22\ \mathrm{s}^{-1}$ at 95 °C which corresponds to a decrease of 2% of its initial thickness. Compared to the temperature effect, the shear effect is much stronger. Such a layer decrease would correspond to a regular temperature variation of 200 °C. It is interesting to remark that the shear induces the monodomain alignment (the 001 intensity increases) but decreases the layer thickness whereas the decrease of temperature improves the smectic order parameter but increases the layer thickness. These comparisons show that the thickness decrease originates from

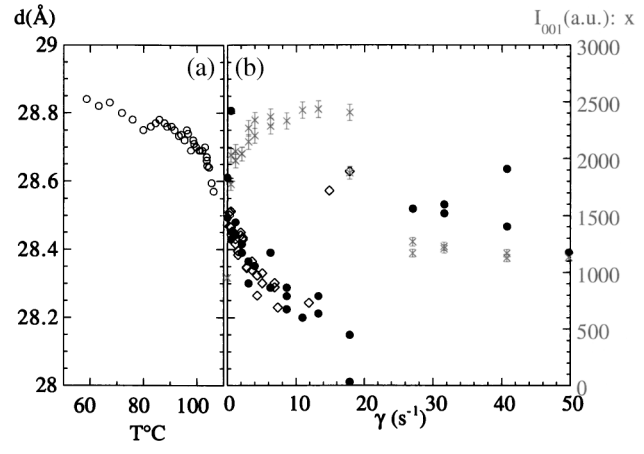

FIG. 2. Evolution of the smectic layer thickness d (Å): (a) (○): versus temperature (and absence of constraint); (b) (●): versus shear rate at 95 °C and completed with (renormalized) values obtained at 90 °C with the multidetector PAXY (◇). The three-axis measurement accuracy is 0.15%. (×) evolution of the 001 smectic reflection (maximum of intensity) at 95 °C versus shear rate. The accuracy on the intensity is 3%.

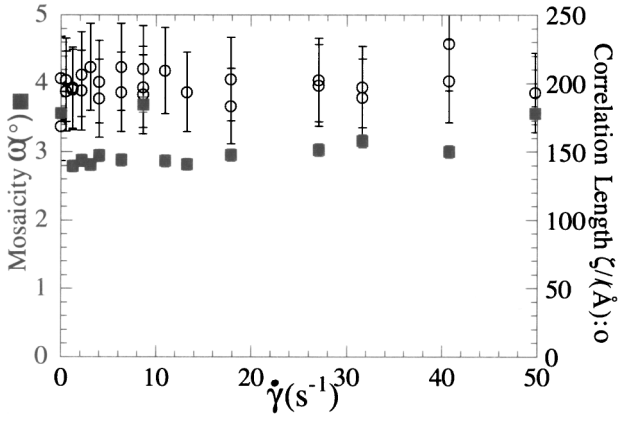

FIG. 3. Evolution of the mosaicity $\omega(^{\circ})$ (■) within the $(\vec{v}, \vec{z})$ plane and the correlation length $\xi_{\parallel}$(Å) along the normal to the layers (○), versus shear rate at 95 °C.

different processes. The characteristic time introduced by the shear process is far too slow to affect just a part of the side mesogen as the alkyl extremity (the local dynamics scales with 10^{-9}–10^{-11} s). We thus conclude that this thickness decrease concerns the whole mesogens and claim that the shear has induced a structural change similar to a S_A-S_C phase transition.

From a theoretical point of view, the detailed approach proposed by Ben Abraham and Oswald [7(a)] and Oswald and Kléman [7(b)] for thermotropic smectics under flow should be suitable for the description of the polymeric smectics. To compensate the variation of distance between the shear plates, the smectic phase is supposed to create new dislocations. These defects are at the origin of an undulation instability. It is interesting to see that the instability proceeds from a dilatation mode (and not compression of the layers). They distinguish two regimes depending on the shear rates. At low shear, the undulation remains stationary. At higher shear, a second undulation is supposed to develop perpendicular to the velocity direction giving rise to a two-dimensional crystal with a dilatation rate varying as a square function of the velocity [7(b)]. Experiments on small molecular weight smectics have confirmed this scheme. Finally, following Ribotta and Durand [7(c)], a compressive stress (without shear) on a smectic A favors rather a layer undulation than a mesogen tilt.

The confrontation with the theoretical model provides effectively an interpretation for the existence of the critical shear rate $\dot{\gamma}_0$ above which a 2D orientation could be developed. However, the hypothetical dilatation process is largely overcome by another phenomenon which is at the origin of the reduction of the layer thickness. In contrast with what could be expected, the shear induced "S_C" phase cannot be assimilated to these undulation instabilities since the normal to the layers $\vec{\ell}$ keeps the same direction as in the S_A phase; i.e., $\vec{\ell}$ is parallel to the $\vec{\nabla} \cdot \vec{v}$ axis. The variation of the layer thickness corresponds to a tilt of 13°. Since the 001 angular position [Fig. 4(a) and [3]] is not modified in these proportions, a tilt of the mesogens which keeps the layer orientation as in the unsheared oriented state is the most probable situation. Such internal rearrangements are all the more surprising that they were never reported for small molecular weight liquid crystals or block copolymers even in the vicinity of phase transitions.

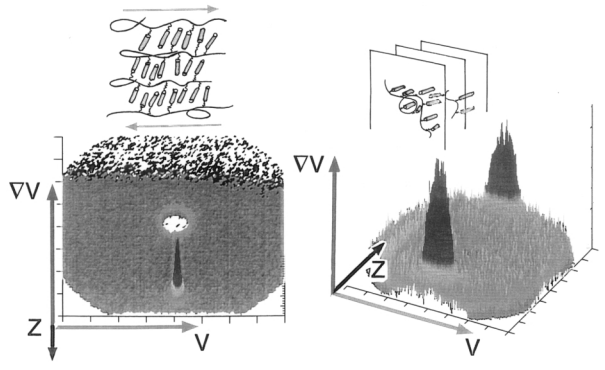

(a) (b)

FIG. 4. Scattering patterns (2D-multidetector PAXY): (a) in the $(\vec{v}, \vec{\nabla} \cdot \vec{v})$ plane for the low molecular weight PMA-OC_4H_9 ($\dot{\gamma} = 0.3\ s^{-1}$, $T = 95$ °C). (b) In the $(\vec{v}, \vec{z})$ plane for the high molecular weight polymer ($\dot{\gamma} = 0.2\ s^{-1}$, $T = 85$ °C). The velocity axis is horizontal.

In this parallel orientation, which corresponds to the low constraint layer orientation (low shear regime), the main chains are supposed to remain mostly confined within two successive mesogenic layers (almost a 2D trajectory). How do we understand that the shear produces the main-chain elongation along the velocity axis and why the S_A modulation is not restored? At low shear, the parallel layer orientation transforms the shear process in a slip motion between the mesogenic layers in which the main chains are stretched. These main chains are engaged in a complex process since the same main chain can participate, via its side chains, to two successive layers subjected to two different velocities. The upper layer motion of higher velocity is partially transmitted via the mesogen interactions to the lower velocity layer. This process is ensured from layers to layers as long as two successive layers contain the mesogens belonging to the same chain. Reciprocally, the stretched main chain exercises a continuous torque on the side mesogen via its fixed extremity. The tilt angle should be *a priori* homogeneous in the whole sample because of the velocity gradient field. A consecutive compression of the whole sample is thus expected; however, the variation of gap between the parallel plates overcomes the variation of thickness (estimated to 5% for a gap of 1 mm) and can be probably neglected. Compared to small molecular weight homologs, the slip process displayed by LC polymers in the parallel orientation involves a direct connection between the successive layers. The chemical linkage to the main chain and the cooperative nature of the interaction along the $\vec{n}$ axis makes appear the force of the main-chain(interlayer)/mesogens coupling which is exacerbated under shear flow. In addition to the usual terms describing the smectics (layer undulations and displacements), the description of the hydrodynamics of the polymeric smectics needs to contain an efficient coupling parameter which takes into account this specific interaction which binds the polymer to the mesogen. Up to now, both experimental and theoretical results have evidenced that the only effects of the mesogen/main-chain coupling in SCLCPs should be, at rest, a strong main-chain anisotropy [5(a)] since these systems are rather dominated by the side-chain ordering. Under shear flow in contrast, we show for the first time that *the polymer main chain is able to induce a change in the liquid crystalline structure,* i.e., the S_A-S_C transition. It is clear that the theoretical approach proposed by Renz and Warner some years ago for SCLCPs at rest [8] should be reconsidered. In low molecular weight homologs, an equivalent interlayer/mesogen coupling is

usually negligible since no tilt is observed. However, very recently, Auernhammer *et al.* [9] have introduced a term which couples the normal to the layers to the director in their theoretical developments of the smectics hydrodynamics. Such an approach is very promising in the frame of the side-chain polymers. The second regime observed at high shear rates ($\dot{\gamma} > \dot{\gamma}_0$) suggests strongly a reorientation of the director towards the neutral axis (perpendicular orientation) as it was already noticed for block copolymers [10]. However, it is open to question to know how to relate the transition to the main-chain elongation and to the layer instability developments. From an experimental point of view, the study of larger angles could provide a complementary description of the local mesogen interaction.

The study of a higher molecular weight side-chain polymer homolog ($M_w = 610\,000$, $I = 2.7$) has confirmed the perpendicular orientation. For this orientation, the $(\vec{v}, \vec{z})$ plane becomes the right plane of observation; Fig. 4(b) is thus measured with the cone-plate geometry [3(a)] and here with the 2D SANS multidetector. The scattering associated to the smectic layers is centered on the neutral axis $\vec{z}$ which means that the normal to the layers $\vec{\ell}$ points in that direction (smectic equivalent of the nematic "log-rolling" geometry). This orientation seems to be reinforced by increasing the shear rate but without any specific layer thickness dependence (Fig. 5); it is indeed a lower constraint geometry. Compared to the parallel orientation, the mosaicity is larger ($\omega \approx 10°$ compared to 3° measured as the half width at half maximum) and could contain two superposed orientations. A detailed description of the perpendicular orientation is not the purpose here; the main information is that the smectic layer orientation is conditioned by the main-chain length. It can be noticed that a chain length influence was also reported in the nematic phase [11]. How does the polymer length govern the layer orientation? In these polymeric smectics, the density of main-chain crossings through the mesogenic layers increases with the molecular weight following a power law $R_{\|} \alpha M^{0.83 \pm 0.03}$, where $R_{\|}$ is the average main-chain extension along the director [5(b)] [and decreases slightly with the temperature [5(a)]]. Under shear flow, these crossing defects become costly if the parallel geometry is conserved because of the slip motion. The slip does not exist anymore in the perpendicular orientation; this geometry is thus favored for a high crossing density and reveals also that the relevant relaxation time is the one of the main-chain crossings.

The study of SCLCPs opens new ways for a better understanding of the rheology of the lamellae systems since it presents the advantage of tailored systems for which the mesogenic interaction can be modulated; the density of defects (layer crossings) is controlled via the molecular weight or the temperature. It is obvious that a systematic study of these systems as a function of the parameters exposed above will provide much information on the mechanisms of orientation of lamellae phases. From a theoretical point of view, it is interesting to note that, whereas the consequences of the liquid crystalline field on the chain geometry have been predicted, the role of the polymer coupling on the stability of the liquid crystalline phase remains mostly unexplored.

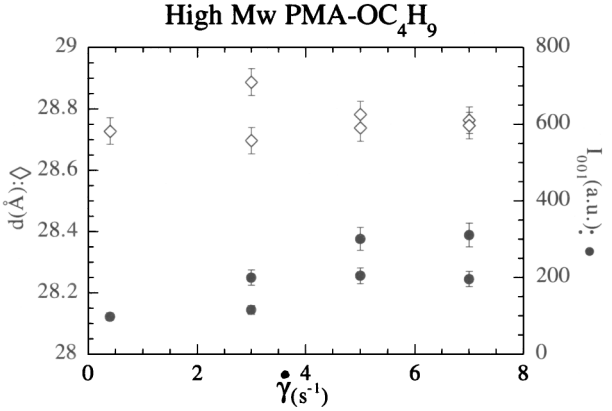

FIG. 5. 001 smectic reflection intensity (◇) and layer thickness d (Å) (●) displayed by the high molecular weight polymer [PAXY measurements—$(\vec{v}, \vec{z})$ plane] versus shear rate.

The author thanks G. Kirsch and S. Lecommandoux for the synthesis, P. Baroni for his technical help, and G. K. Auernhammer for stimulating discussions.

[1] O. Diat, D. Roux, and F. Nallet, J. Phys. II (France) **3**, 1427 (1993); C. R. Safinya, E. B. Sirota, and R. J. Plano, Phys. Rev. Lett. **66**, 1986 (1991).
[2] C. Castelletto, L. Noirez, and P. Vigoureux (to be published).
[3] (a) L. Noirez and A. Lapp, Phys. Rev. E **53**, 6 (1996); (b) Phys. Rev. Lett. **78**, 1 (1997); **78**, 70 (1997).
[4] R. Muller, C. Picot, Y. H. Zang, and D. Froelich, Macromolecules **23**, 2577 (1990).
[5] (a) L. Noirez, G. Pépy, P. Keller, and L. Benguigui, J. Phys. II (France) **2**, 821 (1991); (b) L. Noirez, C. Boeffel, and A. Daoud-Aladine, Phys. Rev. Lett. **80**, 7 (1998); **80**, 1453 (1998).
[6] (a) L. Noirez, P. Davidson, W. Schwarz, and G. Pépy, Liq. Cryst. **16**, 1081 (1994) (Fig. 1 therein corresponds to the polymer deuterated on the main chain); (b) P. Davidson and A. M. Levelut, Liq. Cryst. **11**, 469 (1992).
[7] (a) S. I. Ben Abraham and P. Oswald, Mol. Cryst. Liq. Cryst. **93**, 383 (1983); (b) P. Oswald and M. Kléman, J. Phys. (Paris), Lett. **43**, L-411 (1982); (c) R. Ribotta and G. Durand, J. Phys. (Paris) **38**, 179 (1977).
[8] W. Renz and M. Warner, Proc. R. Soc. London A **417**, 213 (1988).
[9] G. K. Auernhammer, H. R. Brand, and H. Pleiner, Rheol. Acta (to be published).
[10] K. A. Koppi, M. Tirrell, F. S. Bates, K. Almdal, and R. H. Colby, J. Phys. II (France) **2**, 1941 (1992).
[11] S. F. Rubin, R. M. Kannan, J. A. Kornfield, and C. Boeffel, Macromolecules **28**, 3521 (1995).